remote sensing

MDPI

Article

Spatiotemporal Landscape Pattern Analyses Enhanced by an Integrated Index: A Study of the Changbai Mountain National Nature Reserve

Ying Zhang [1], Jingxiong Zhang [2,*], Fengyan Wang [1] and Wenjing Yang [3]

[1] College of Geo-Exploration Science and Technology, Jilin University, Changchun 130026, China
[2] School of Geodesy and Geomatics, Wuhan University, Wuhan 430079, China
[3] College of Geography and Environment, Shandong Normal University, Jinan 250358, China
* Correspondence: jxzhang@whu.edu.cn

Abstract: The analysis of spatiotemporal changes of landscape patterns is of great significance for forest protection. However, the selection of landscape metrics is often subjective, and existing composite landscape metrics rarely consider the effects of spatial correlation. A more objective approach to formulating composite landscape metrics involves proper weighting that incorporates spatial structure information into integrating individual conventional metrics selected for building a composite metric. This paper proposes an integrated spatial landscape index (ISLI) based on variogram modeling and entropy weighting. It was tested through a case study, which sought to analyze spatiotemporal changes in the landscape pattern in the Changbai Mountains over 30 years based on six global land-cover products with a fine classification system at 30 m resolution (GLC_FCS30). The test results confirm: (1) spatial structure information is useful for weighting conventional landscape pattern metrics when constructing ISLI as validated by correlation analysis between the incorporated conventional metrics and their variogram ranges. In terms of the range parameters of different land cover types, broadleaf forest and needleleaf forest have much larger range values than those of other land cover types; (2) DIVISION and PLAND, two of the conventional landscape metrics considered for constructing ISLI, were assigned the greatest weights in computing ISLI for this study; and (3) ISLI values can be used to determine the dominant landscape types. For the study area, ISLI values of broadleaf forests remained the largest until 2020, indicating that forest landscape characteristics were the most prominent during that period. After 2020, the dominance of needleleaf forest gradually increased, with its ISLI value reaching a maximum of 0.91 in 2025. Therefore, the proposed ISLI not only functions as an extension and complement to conventional landscape metrics but also provides more comprehensive information concerning landscape pattern dynamics.

Keywords: landscape pattern metrics; integrated spatial landscape index (ISLI); variogram; entropy; spatial correlation; Changbai Mountain National Nature Reserve

Citation: Zhang, Y.; Zhang, J.; Wang, F.; Yang, W. Spatiotemporal Landscape Pattern Analyses Enhanced by an Integrated Index: A Study of the Changbai Mountain National Nature Reserve. *Remote Sens.* **2023**, *15*, 1760. https://doi.org/10.3390/rs15071760

Academic Editors: Roshanak Darvishzadeh and Dimitrios D. Alexakis

Received: 6 March 2023
Revised: 17 March 2023
Accepted: 22 March 2023
Published: 24 March 2023

1. Introduction

Since the 21st century, the study of landscape patterns has gradually tended toward the analysis of landscape spatial heterogeneity [1,2], and the research field has grown rapidly [3,4]. A landscape pattern is defined as spatial arrangements of various landscape elements in a range of sizes and shapes [5,6]. Landscape pattern analysis [7,8] is used to detect and describe observed structures in landscape features (most commonly land cover) or land use (e.g., urbanization). Following this approach, various landscape metrics, also known as spatial pattern metrics, spatial pattern indices, or landscape pattern metrics, are proposed and used to quantify and analyze landscape patterns [9,10]. As measurable units of landscape composition and acting as a surrogate for change, they allow for the description and quantification of spatial patterns and ecological processes over both space

and time [3]. The ultimate goal of these analyses is not only to describe these patterns but also to correlate them with the underlying ecological processes driving them.

Given numerous existing landscape metrics, it is also important to assess and select landscape metrics well suited for an area or an application purpose. Several methods have been developed for this, such as analytic hierarchy process (AHP) [11], fuzzy comprehensive evaluation (FCE) [12], and entropy weighting [13]. AHP is widely used for selecting the related landscape indicators and metrics. The problem of the quantification of a large number of uncertain factors can be well solved by FCE. However, both AHP and FCE are subjective assessment methods, with the former's hierarchical structure and the latter's different levels of multiple factors not suitable for land cover pattern analyses, as seen in this study. Entropy weighting, being an objective weighting method for ecological assessment studies, determines a pattern index's weight according to its information entropy and has been increasingly used in research [14]. According to Shannon's view [15], information entropy measures the disorder degree of a landscape index. A landscape index with higher information entropy is equivalent to its higher variation and greater contribution to the whole system, leading to a larger weight [16].

Landscape pattern metrics are often of different orders of magnitude in terms of values and may well be correlated, while the changes in the characteristics of the overall landscape may also be correlated. To comprehensively describe the overall landscape patterns and changes, different integrated landscape metrics have been proposed. Liu et al. [6] proposed a landscape expansion index (LEI) for quantifying urban expansion and capturing the information about the formation processes of a landscape pattern using multi-temporal remotely sensed data. Zhang et al. [17] constructed the integrated landscape index (ILI) for analyzing the overall landscape pattern of different shores in coastline mangrove forests in China. Zou et al. [18] introduced a landscape fragmentation index (LFI) to assess and analyze the spatiotemporal heterogeneity of China's landscape fragmentation from 1980 to 2020.

However, the selection of landscape metrics is often subjective, and existing composite landscape metrics rarely consider the effects of spatial correlation. In this study, we propose an integrated spatial landscape index (ISLI) based on variogram range parameters and entropy weighting and use it to analyze the landscape patterns of Changbai Mountain Reserve, China, the study area chosen, more comprehensively. Experiments using six global land cover products were carried out to analyze landscape pattern changes using the proposed integrated metric as opposed to several conventional indices incorporated for constructing ISLI.

The analyses were focused on: (i) highlighting the added values of ISLI, which can identify the important landscape type, describe landscape pattern dynamics more comprehensively than conventional landscape metrics and transition matrices, and retain the descriptive functionality of conventional landscape metrics integrated by ISLI; (ii) confirming the validity of information entropy-based weighting for constructing ISLI through variogram modeling and correlation analysis (which is between conventional landscape pattern metrics selected in constructing ISLI and their variogram range parameters); and (iii) explaining the distinctions and linkages of ISLI to the conventional landscape metrics selected for constructing ISLI.

The paper is organized as follows. In Section 2, the study area and methods for constructing ISLI are described. Experiments with six global land cover maps are presented in Section 3 where the experimental results and discussion are presented along with experimental procedures. This is followed by some concluding remarks.

2. Materials and Methods

2.1. The Study Area and Datasets

The Changbai Mountain National Nature Reserve is located in the southeast of Jilin Province (at 41°35′N–42°25′N, 127°40′E–128°16′E), and it is the most representative temperate forest in the northern part of the northern hemisphere. It is the world's largest

temperate virgin forest reserve in the same latitude and also one of the most completely preserved forest ecosystems in the world [19]. Its climate is characterized by cold weather during the long winter and short, cool summers. Its annual mean temperatures range from –7 °C to 3 °C [20]. Its elevations are between 624 and 2694 m above sea level with slope gradients ranging from 0 to 70 degrees. It is known as the "China Water Tower" and is home to a renowned ecological museum that is rich in natural resources. In addition, it is crucial for controlling northeast China's climate change. As forest land is the main body of this terrestrial ecosystem, the security of its forest ecosystem is an important mission in the construction of the "China-Mongolia-Russia Economic Corridor" of the "Belt and Road" initiative. Figure 1 is an overview of the study area, in which Figure 1a is the geographic location map of the Changbai Mountain National Nature Reserve, and Figure 1b,c are the DEM map and slope map of this area, respectively.

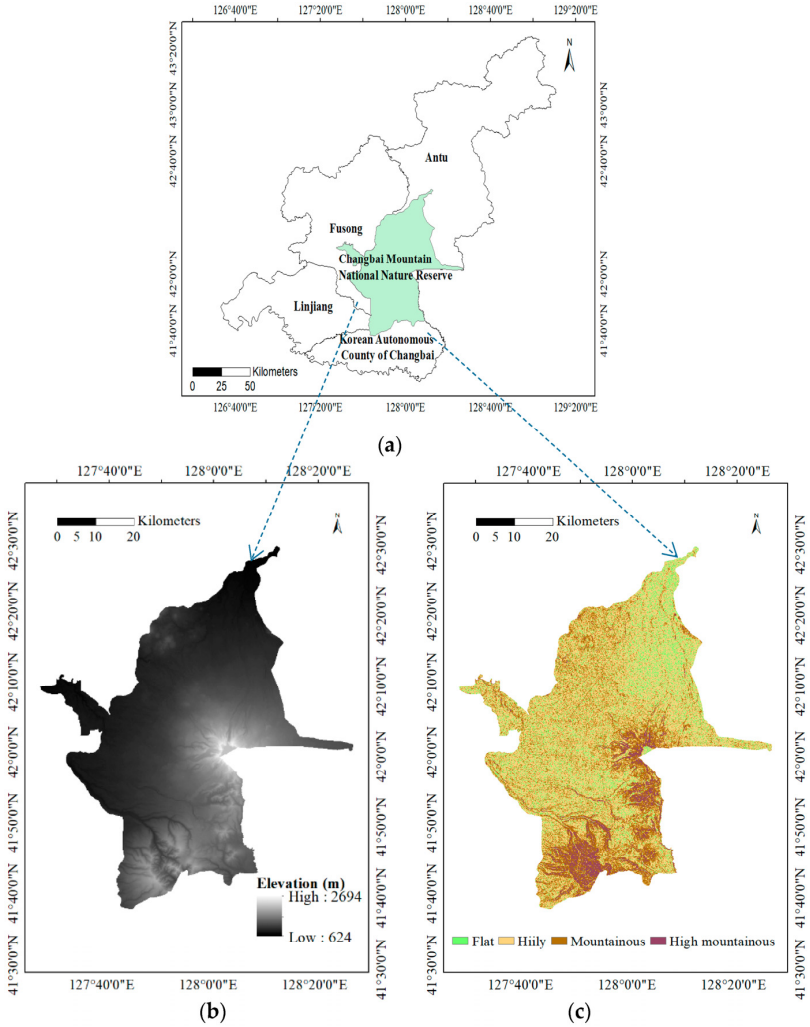

Figure 1. Overview of the Study Area: (**a**) geographic location of the study area, (**b**) DEM, and (**c**) slope map.

Concerning the study area, there is currently a lack of research regarding its long-term landscape pattern analyses. Given that it is an area rich in natural resources, is environmentally and socially significant, and more importantly, is representative in terms of forest landscape pattern dynamics, it was chosen as the study area, where it is appropriate to test the validity of the proposed integrated landscape metrics.

The classification map used in this study is the Global Land Cover with a fine classification system at 30 m, which is provided by the Data Sharing and Service Portal [21],

Chinese Academy of Sciences. The producer accuracy and user accuracy of its forest products are superior to other similar 30 m global forest products [22,23]. As the products cover a longer period, it is convenient for time series analysis. When compared with the dominant land cover types in the study area, some land cover types are underrepresented and therefore merged. This led to six major land cover types, including cropland, broadleaf forest, needleleaf forest, mixed leaf forest, impervious surface, and water body, as shown in Figure 2.

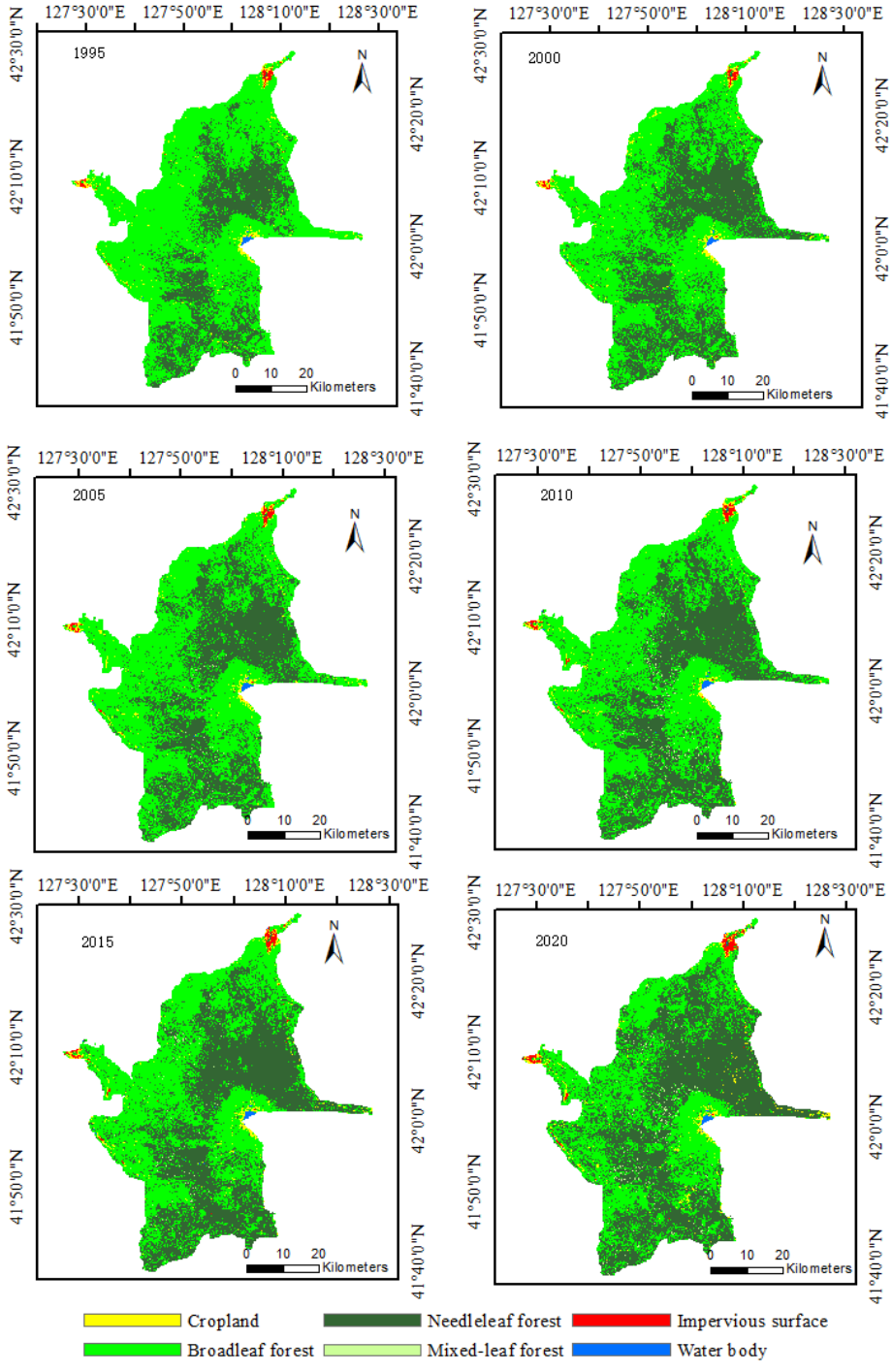

Figure 2. Land Cover Map of the Study Area from 1995 to 2020.

2.2. An Integrated Spatial Landscape Index (ISLI)

The proposed ISLI seeks to describe spatiotemporal changes in landscape patterns by integrating certain selected conventional landscape metrics based on information entropy and variogram modelling to provide a more comprehensive view of the areas under study. The weighting strategy is based on information entropy, which is itself based on correlation analyses between individual landscape metrics and their variogram ranges.

Entropy weighting is based on the concept of Shannon entropy [15]. The greater the information entropy of a landscape index (the greater the amount of information it provides), the larger the weight given to the landscape index and vice versa. The method of entropy weighting for landscape metrics works in three main steps: normalization, information entropy calculation, and weight calculation.

Normalization is based on the correlation between landscape metrics and their variogram range parameters. A landscape index is positively or negatively weighted, depending on the results of correlation analysis. A landscape index positively correlated with the range is a positive normalization index; otherwise, it is a negative normalization index, as shown in Equation (1):

$$\begin{aligned} \text{positive normalization index}: \ Z'_{kq} &= \frac{\left(Z_{kq} - \min\left(Z_q\right)\right)}{\left(\max\left(Z_q\right) - \min\left(Z_q\right)\right)} \\ \text{negative normalization index}: \ Z'_{kq} &= \frac{\left(\max(Zq) - Z_{kq}\right)}{\left(\max(Zq) - \min(Zq)\right)} \end{aligned} \tag{1}$$

where Z_{kq} referes to the kth year and the qth landscape index; Z'_{kq} is the normalized landscape index; and $\max\left(Z_q\right)$ and $\min\left(Z_q\right)$ are the maximum and minimum values of the qth index, respectively. Since entropy weighting uses logarithmic operation, the normalized value needs to be added to a small positive number:

$$Z''_{kq} = Z'_{kq} + A \tag{2}$$

where $A = 0.01$ in this paper.

To compute information entropy of an index say q, we need to calculate its weight in the kth year, i.e.,

$$p_{kq} = {}^{Z''_{kq}}/_{\sum_{k=1}^{n} Z''_{kq}} (k = 1, 2, \cdots, l; q = 1, 2, \cdots, m) \tag{3}$$

where l is the number of years for analysis and m is the number of landscape index. Then, the information entropy of index q, H_q, is calculated as:

$$H_q = -b\sum_{k=1}^{l} p_{kq} ln\left(p_{kq}\right) \tag{4}$$

where b is an adjustment coefficient, calculated as $b = 1/ln(l)$.

The weight of landscape index q is:

$$w_q = \frac{1 - H_q}{m - \sum_{q=1}^{m} H_q} \tag{5}$$

ISLI is then computed as:

$$\text{ISLI} = w_q \times Z''_{kq} \tag{6}$$

As mentioned above, variogram range parameters are required for judging the positive and negative effects of the landscape metrics incorporated for constructing ISLI. A variogram is defined as the variance of the difference between values of a regionalized variable at two locations and characterizes the spatial continuity of a dataset. The parameters of a theoretical model include sill, nugget, and range. Range indicates the distance beyond

which observations are uncorrelated and represents the lag distance when the variogram reaches its maximum value [24]. The range parameter thus indicates the range of spatial correlation of the underlying variable [25]. If the value of the range is big, it means that the land cover type has a bigger range of spatial correlation and similar spatial features over a larger distance and vice versa [26–28].

A flowchart is presented in Figure 3. To provide a quick review of the study area, land use transition matrices of different land cover types in the Changbai Mountains from 1995 to 2020 were first built. Second, landscape metrics of various land cover products in each period were calculated, with the appropriate landscape metrics determined for the study area based on their statistical correlation results. Third, through variogram modeling of different land cover types, the spatial structure of land cover types in the Changbai Mountain area was further studied. Moreover, Pearson's correlation analyses between the range parameters and landscape metrics were analyzed, while ISLI was constructed based on entropy weighting. Finally, conclusions were drawn about the dynamic changes of the landscape pattern in the Changbai Mountain National Nature Reserve.

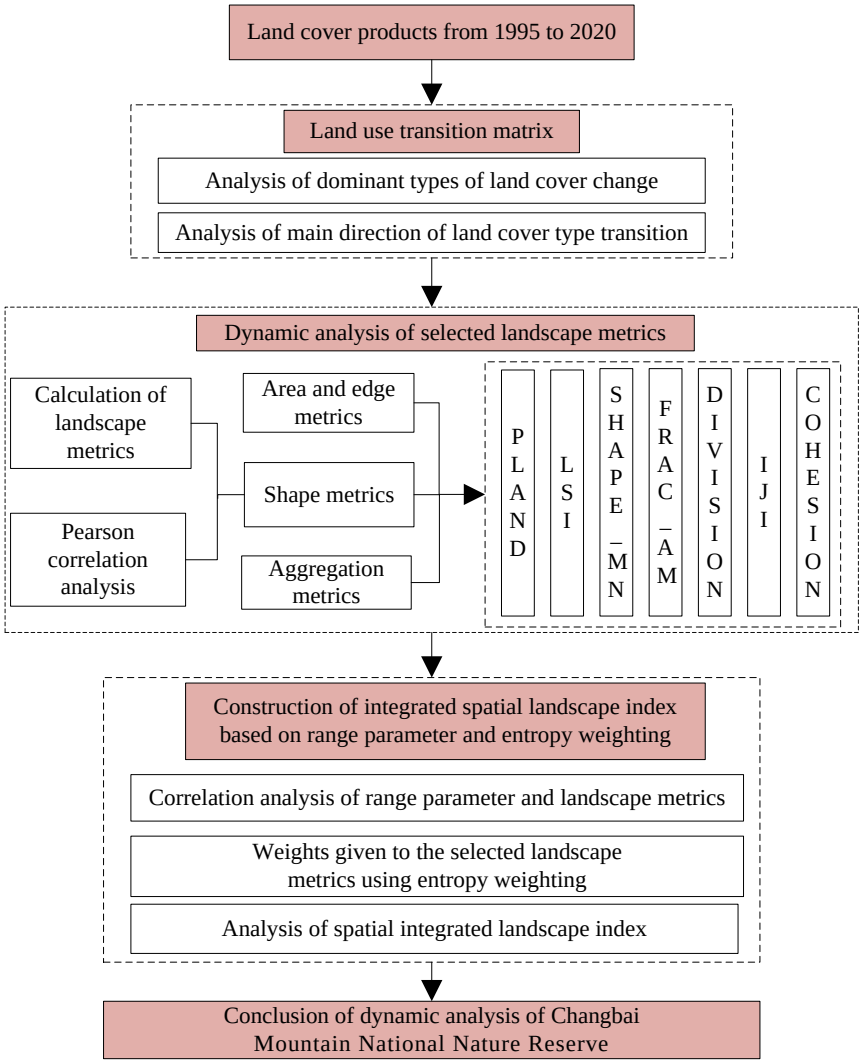

Figure 3. Technical Flow Chart.

3. Results and Discussion

3.1. Land Cover Change

Figure 4 shows the major land cover changes in the Changbai Mountain Reserve from 1995 to 2020. We exclude minor land cover change types (less than 10,000 pixels) to show

major changes. The gray areas are the unchanged areas, the yellow areas with the most prominent change are the conversion areas from broadleaf forest to needleleaf forest, and the black areas with less prominent change are the conversion areas from needleleaf forest to broadleaf forest. Therefore, broadleaf and needleleaf forest represent the dominant types of land cover change. The amount of grassland in the study region is so minimal that it was also classed as cropland, which is why the long, narrow strip bordering North Korea to the east has increased cropland.

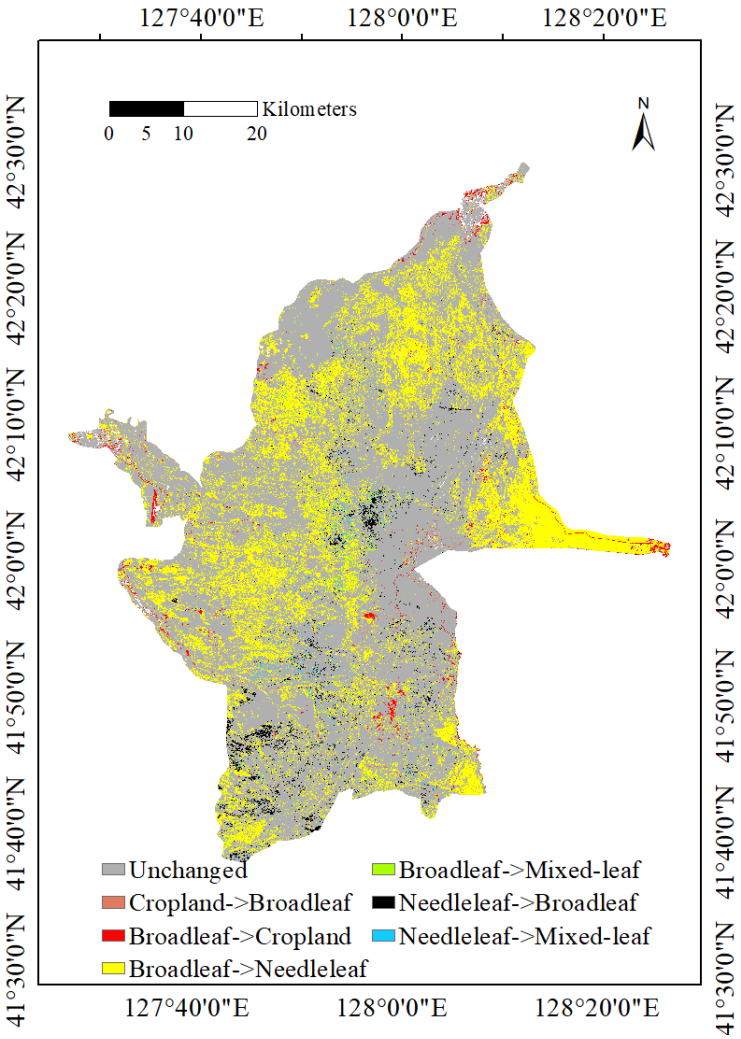

Figure 4. Major changes in land cover types of Changbai Mountain Reserve from 1995 to 2020.

Land cover transition reflects land use transition and has important ecological and social implications. Therefore, the land use transition matrix is often used to analyze the characteristics and change trends of landscape structures at different times [29]. The heat maps of the transition matrices of the Changbai Mountains from 1995 to 2020 are shown in Figure 5. For more information, see Table A1 in Appendix A. From 1995 to 2000, the newly added needleleaf forest mainly resulted from the conversion of 399.09 km^2 of broadleaf forest, and the special treatment for mixed leaf forest led to its high conversion rate. From 2000 to 2010, the conversion ratio of cropland was as high as 35.7%, and it mainly became broadleaf forest. Needleleaf forest gains mainly resulted from the conversion of broadleaf forest. From 2010 to 2020, the newly added area of cropland was mainly due to the conversion of 17.65 km^2 and 16.31 km^2 of broadleaf forest. Although a small amount of cropland was also converted into broadleaf forest, and more broadleaf forest was converted into needleleaf forest, resulting in a significant decrease in its total area. Only from 2015

to 2020 were there minor percentage changes in the impervious surface, while there was no conversion from 1995 to 2015. Combining the results in Figures 4 and 5, it can be seen that the large increase in cropland and needleleaf forest is mainly due to the conversion of broadleaf forest, while cropland is also converted into broadleaf forest and impervious surface in a small amount. Therefore, the transition from broadleaf forest to cropland and needleleaf forest is the main transition type in this period, and the shrinking of broadleaf forest and the expansion of needleleaf forest are the main transition trends in this period.

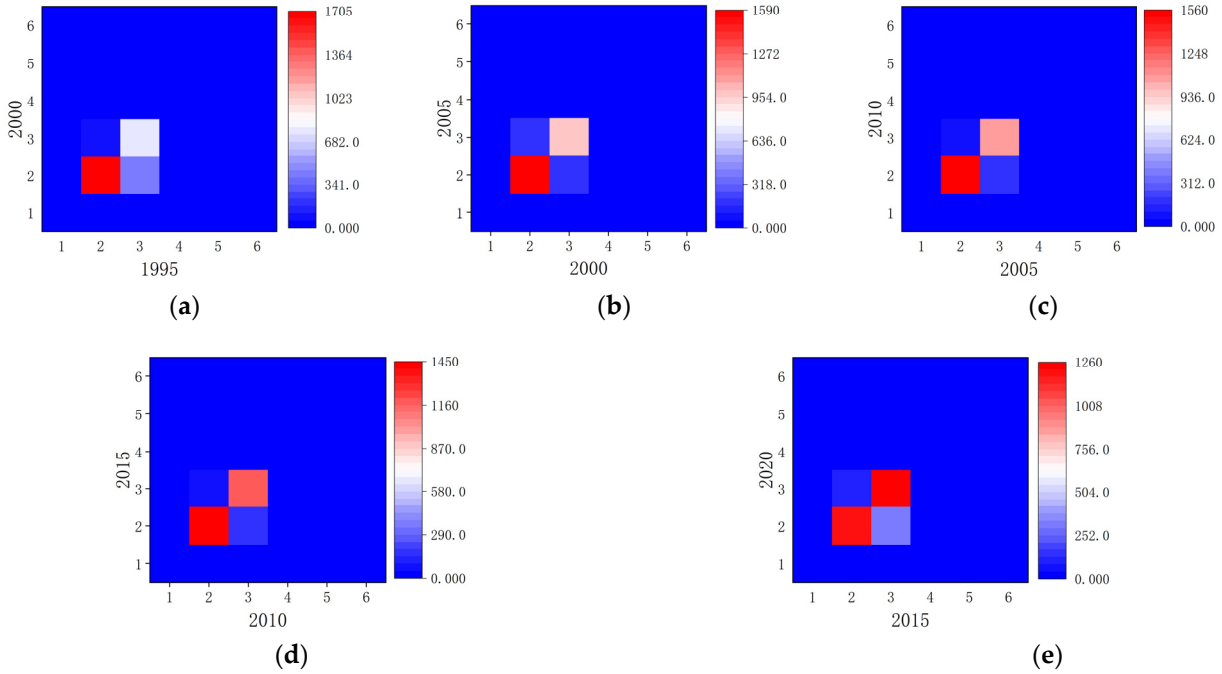

Figure 5. Heat maps of the transition matrices of the Changbai Mountains from 1995 to 2020 (unit: km^2): (**a**) from 1995 to 2000, (**b**) from 2000 to 2005, (**c**) from 2005 to 2010, (**d**) from 2010 to 2015, and (**e**) from 2015 to 2020.

For further verification, the CA-Markov model, which has the characteristics of high simulation accuracy and the visualization of the spatial distribution pattern [30,31], was chosen to predict the land cover types in 2025. This method is based on the MARKOV and CA-MARKOV modules in the software IDRISI, which is a raster-based spatial analysis software developed by Clark Labs at Clark University. The 2010 and 2015 LC maps were used to predict the 2020 LC maps. The Kappa statistics between the reference and predicted 2020 LC maps was 0.885, indicating that the CA-Markov model can be used to simulate land cover change in the study area with high accuracy. The probability and transition matrix between the 2015 and 2020 maps were then used as inputs into the CA-Markov model to simulate land cover in 2025. The prediction result is shown in Figure A1, Appendix B. Nevertheless, the side effects of using simulated maps in landscape pattern analysis should be noted when interpreting the results.

3.2. Landscape Metrics of Different Land Cover Types

Landscape metrics reflect landscape structures and quantitatively describe spatial characteristics. Remote sensing images, which serve as the information carrier for the landscape pattern, can express information about the landscape pattern efficiently and quantitatively [32]. The specific landscape metrics employed for this study are shown in Appendix C (see Table A2). Based on the characteristics of the study area, this paper focuses on analyzing the spatial pattern of the landscape in terms of quantity, shape characteristics, and aggregation [33].

FRAGSTATS 4.2 is currently the most frequently used landscape index calculation software, which can be used to quantify landscape structure. Due to the existence of a large number of redundant landscape metrics that are not relevant to the study, landscape metrics are selected according to the following three principles [17,34]: (a) whether the landscape index has clear ecological significance; (b) whether the landscape index can reflect the landscape pattern characteristics within the study area; and (c) to ensure low redundancy among those selected. According to the above principles, we used Pearson's correlation analysis to evaluate the relationship between the landscape metrics in Appendix D (see Tables A3–A5). In statistics, the covariance of two sets of data is generally divided by the standard deviation of the corresponding data series to obtain Pearson's correlation coefficient [35,36]. If the absolute value of the correlation coefficient is greater than 0.75, then there is a significant correlation (at the significance level of 0.01) between the landscape metrics [37].

Seven landscape metrics were determined, including PLAND, LSI, SHAPE_MN, FRAC_AM, DIVISION, IJI, and COHESION. The values of the landscape metrics are shown in Figure 6. PLAND quantifies the proportional abundance of each patch type in the landscape. The PLAND values of broadleaf forest and needleleaf forest mean that the two land cover types dominated the landscape. LSI provides a standardized measurement of the total edge or edge density that adjusts for the size of the landscape and reflects the complexity of the overall landscape. The LSI values show that the landscape shapes of impervious surfaces and water bodies are relatively regular, while broadleaf forest and needleleaf forest are more complex. SHAPE_MN offers a fundamentally patch-centric perspective of the landscape structure, which can reflect the human disturbance and complexity of the landscape. The SHAPE_MN values of cropland are the largest, and this means that cropland is most affected by human beings and has the highest shape complexity compared with other land cover types. FRAC reflects shape complexity across a range of spatial scales (patch sizes), and FRAC_AM weights FRAC by patch area, revealing the fractal rules of the landscape. The values of FRAC_AM are the largest for broadleaf forest and needleleaf forest, indicating that the two have the most complex geometric shapes and the least human interference. Division is interpreted as the probability that two randomly chosen pixels in the landscape are not situated in the same patch of the corresponding patch type and characterizes the fragmentation of the landscape distribution. It can be seen from DIVISION values that the separation degree of broadleaf forest is increasing and that of needleleaf forest is decreasing. Compared with the other four land cover types, the spatial distribution of broadleaf forest and needleleaf forest are more concentrated. IJI emphasizes the degree of adjacency to other adjacent patch types. IJI emphasizes the degree of adjacency to other adjacent patch types. The IJI values of cropland and water body are the largest, indicating that they are more adjacent to other land cover types of patches, while needleleaf forest and broadleaf forest are less adjacent to other types. COHESION is used to quantify the natural connectivity of landscape patches, thus reflecting the level of heterogeneity in the landscape. The COHESION values of broadleaf forest and needleleaf forest are the largest, which further indicates that the two land cover types are dominant land cover types with the largest natural connectivity and the most concentrated distribution.

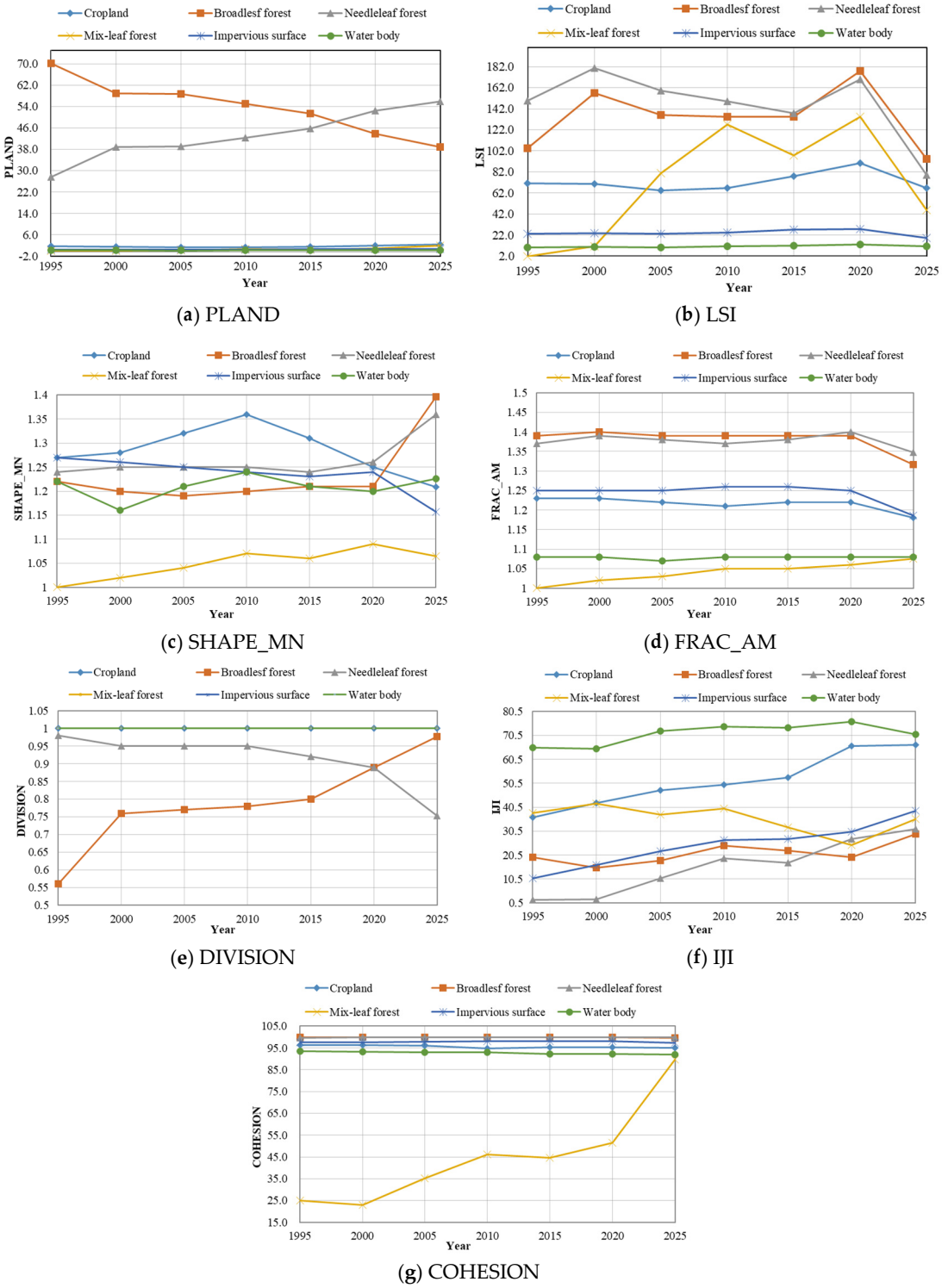

(**a**) PLAND (**b**) LSI

(**c**) SHAPE_MN (**d**) FRAC_AM

(**e**) DIVISION (**f**) IJI

(**g**) COHESION

Figure 6. Dynamic Line Charts of Landscape Metrics for Different Land Cover Types.

3.3. Variogram Structure Analysis

The common theoretical variogram fits the function model: spherical model, exponential model, Gaussian function model, and logarithmic function model. Regionalized variables of a variogram are selected from existing theoretical models. According to the weighted fitting strategy in the sense of least squares and the number of point pairs as weight coefficients, this paper determines that the fitting model used is a nested structure, that is, a free combination structure of a nugget model with an exponential model, spherical

model, or a Gaussian model. The geostatistical modeling of mixed leaf forest could not be performed because the area between 1995 and 2005 was too small (see Table A1 in Appendix A for details). Broadleaf forest and needleleaf forest are the dominant landscapes in the study area, and because there are too many variogram parameters (five land cover types with six periods, and each land cover type has three variogram parameters, for a total of ninety parameters), and therefore, Table 1 simply includes a list of the variogram parameters of the two dominant land cover types, and the nested structure of the nugget model and exponential model are used to fit the data. The variograms of five typical land cover types in the Changbai Mountain Reserve in 2020 are shown in Appendix E (see Figure A2). As the lag distance h of the abscissa increases, the variation degrees of typical land cover types increase significantly. When the abscissa reaches the parameter range, the ordinate of the variogram tends to be in a stable state, indicating that the overall fitting effect is adequate.

Table 1. Fitting Parameters of Variograms for Broadleaf Forest and Needleleaf Forest.

Year	Land Cover Type	Nugget Model	Exponential Model	
		Nugget	Sill	Range
1995	Broadleaf	0.32	0.28	3576.6
	Needleleaf	0.29	0.31	3847.8
2000	Broadleaf	0.30	0.34	3636.0
	Needleleaf	0.30	0.33	4002.6
2005	Broadleaf	0.30	0.35	3933.0
	Needleleaf	0.26	0.36	3819.6
2010	Broadleaf	0.31	0.34	4049.7
	Needleleaf	0.30	0.33	4073.7
2015	Broadleaf	0.28	0.32	4194.6
	Needleleaf	0.29	0.31	5243.4
2020	Broadleaf	0.38	0.32	4073.7
	Needleleaf	0.39	0.29	3556.5

Figure 7 shows range parameters for different land cover types from 1995 to 2020. The ranges of broadleaf forest and needleleaf forest are much higher than those of the other three land cover types, reflecting that the two land cover types have bigger spatial structure sizes and similar features. The main reason is that both are dominant landscapes in the study area, spread throughout the study area, and their spatial aggregation is the largest, so the range values are more reliable. Moreover, the water body area type is almost homogeneous under normal circumstances and should be relatively smooth. However, due to its small overall coverage area and dispersion, except in the Changbai Mountain Tianchi area, the range values are smaller than those of broadleaf forest and needleleaf forest. Furthermore, the ranges of cropland are the smallest among all land cover types. This means that this type ranges has the smallest spatial structure size and is the most complex. Although the total area of cropland is larger than that of impervious surface, as shown in Table A1 in Appendix A, the spatial structure of cropland is more complex due to its scattered and fragmented distribution, while the structure of impervious surface is relatively concentrated.

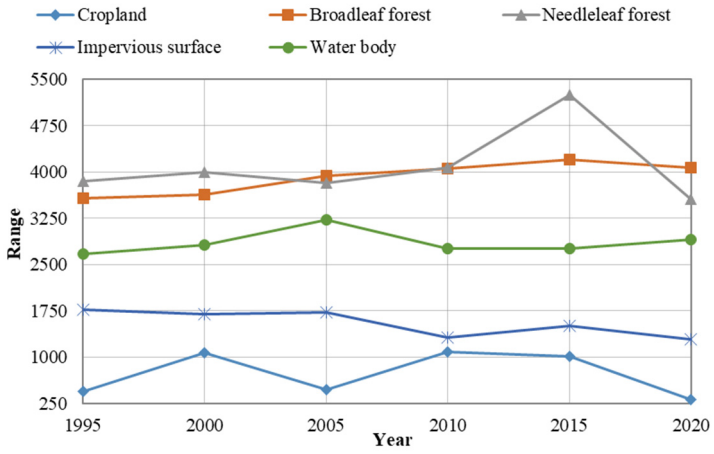

Figure 7. Range Parameters for Different Land Cover Types from 1995 to 2020.

3.4. Analysis with the Proposed ISLI

The calculation of ISLI starts with variogram modelling (which is described in Section 3.3), followed by a correlation analysis between landscape metrics and their correlation ranges. Table 2 shows Pearson's correlation coefficients. Since there are five land cover types over a period of six years participating in correlation analysis, the degree of freedom of the correlation coefficient significance test is 30. When the significance level $\alpha = 0.01$, range parameters were significantly positively correlated with PLAND, LSI, and FRAC_AM but significantly negatively correlated with SHAPE_MN and DIVISION. When the significance level $\alpha = 0.05$, range parameters were significantly positively correlated with COHESION but significantly negatively correlated with IJI. Therefore, there is a statistically significant correlation (either positive or negative) between range parameters and the selected landscape metrics, which were further used to construct the proposed composite index ISLI. It is evident from Table 2 that the area ratio to the landscape, the landscape complexity, and the degree of aggregation all affect how big and complicated the spatial correlation range (spatial structure size) in the region is. The range of spatial correlation is less where the patches are scattered with different neighboring patch types.

Table 2. Pearson's Correlation Coefficients of Range Parameters and Selected Landscape Metrics.

Index	PLAND	LSI	SHAPE_MN	FRAC_AM	COHESION	DIVISION	IJI
Correlation coefficient	0.774 **	0.595 **	−0.568 **	0.490 **	0.461 *	−0.543 **	−0.370 *

** The correlation is significant at the 0.01 level (double tail); * The correlation is significant at the 0.05 level (double tail).

The estimated correlation coefficients shown in Table 2 were used to assess the positivity or negativity of the specified landscape metrics, as described in Equation (1). The entropy based weighting method described in Section 2.2 was applied to calculate the weights of landscape pattern metrics selected, allowing for computing ISLI using Equation (6). Figure 8 shows the results of weights for different land cover types from 1995 to 2025. Since the degrees of dispersion of DIVISION and PLAND are greater, their weights are larger. Table 3 shows Pearson's correlation coefficients between ISLI and the selected landscape pattern metrics, indicating that DIVISION and PLAND are the most crucial metrics in comprehending ISLI. The ideal forest landscape model in the study area should have a large proportion of forest to the total area, a large degree of natural connectivity, a significant agglomeration of spatial distribution, and high overall landscape complexity, as indicated by PLAND, LSI, COHESION, and DIVISION, respectively. As a result, the proposed ISLI seems to be able to retain the descriptions concerning the landscape pattern by the conventional landscape metrics incorporated in the construction of ISLI due to its

high (positive or negative) correlation with PLAND, LSI, COHESION, and DIVISION. Moreover, the positive and negative correlations between the selected landscape metrics and ISLI are consistent with what can be seen when examining the results in Tables 2 and 3.

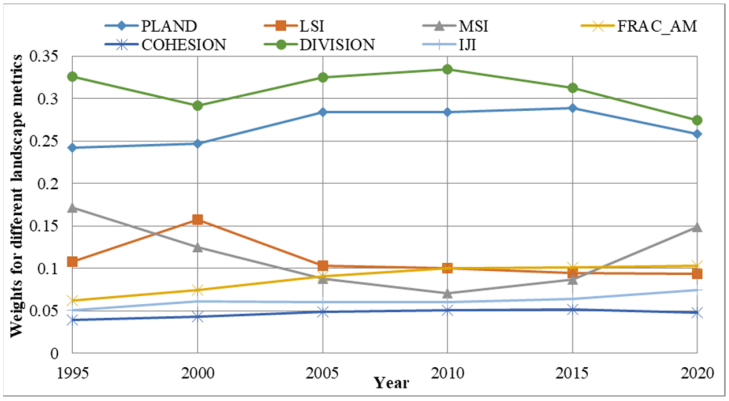

Figure 8. Results of Weights for Different Land Cover Types from 1995 to 2025.

Table 3. Pearson's Correlation Coefficients of ISLI and Selected Landscape Metrics.

Index	PLAND	LSI	SHAPE_MN	FRAC_AM	COHESION	DIVISION	IJI
Correlation coefficient	0.972 **	0.793 **	−0.030 **	0.715 **	0.742 *	−0.830 **	−0.698 *

** The correlation is significant at the 0.01 level (double tail). * The correlation is significant at the 0.05 level (double tail).

There is a question regarding whether the weights obtained from the study area can be generalized to the other zones. The weights are influenced by the landscape metrics chosen for constructing ISLI, by their range parameters, and by the correlations between them. If two zones have similar landscape patterns and the same kinds of land cover types, it is likely that the landscape metrics, their range parameters, the correlation between the metrics and their ranges, and, thus, their weights, would be similar. In this case, the weights calculated for an area may be transferrable between similar landscapes. Otherwise, matrices weights should be calculated anew to further determine the corresponding ISLI values.

Figure 9 shows the results of ISLI for different land cover types. It can be seen that ISLI values of broadleaf forest and needleleaf forest are greater than those of other land cover types, indicating that the two have the most concentrated spatial distribution, are naturally connected, and have the lowest proximity to other patches during the relevant years. On the other hand, other land cover types have smaller ISLI values, meaning that their spatial distributions are relatively scattered and complex.

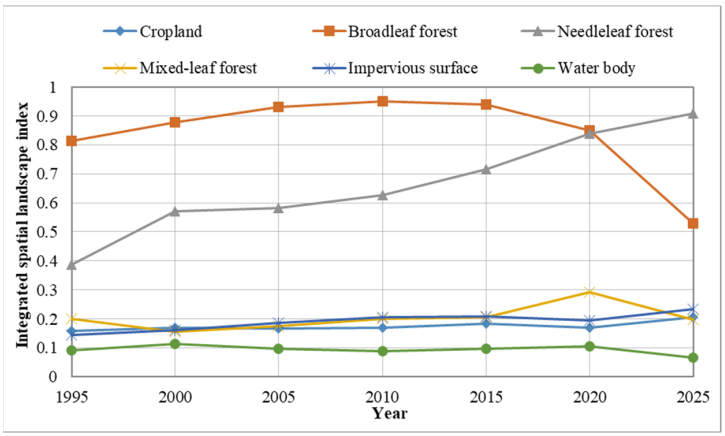

Figure 9. Results of ISLI for Different Land Cover Types from 1995 to 2025.

Although the shrinking of broadleaf forest and the expansion of needleleaf forest are the main trends of land cover change, and the area of needleleaf forest exceeded that of broadleaf forest after 2020, the ISLI values of broadleaf forest were still the largest until 2020, indicating that its landscape characteristics were the most dominant. Moreover, from 1995 to 2025 (as expected), the ISLI values of needleleaf forest were on the rise (ranging from 0.39 to 0.91), indicating that its spatial distribution was more concentrated, the landscape complexity was greater, the natural connectivity was higher, and its dominance in landscape pattern characteristics was larger. From 2020 to 2025, the landscape dominance of needleleaf forest can be seen to gradually increase and the ISLI values of needleleaf forest will reach a maximum in 2025. Although the ISLI values of broadleaf forest range from 0.94 to 0.52 from 2015 to 2025, showing a downward trend, its values are still much higher than those of other land cover types, except needleleaf forest. Therefore, the proposed ISLI can identify the dominant landscape types in specific periods and is more informative than individual landscape metrics (e.g., PLAND).

Considering the area of mixed leaf forest in Table A1 in Appendix A, it can be seen that this area is gradually increasing, but in terms of ISLI, the slow increase of this type does not significantly change the status of its landscape. Furthermore, although the COHESION values of mixed leaf forest in Figure 6g shows a significant upward trend and COHESION is a positive normalization index, as shown in Table 2, its weights are too small, resulting in no substantial change in its ISLI values. Impervious surface is mainly distributed in three separate economic management areas, including the Chibei (north of the Changbai Mountains), Chixi (west of the Changbai Mountains), and Chinan (south of the Changbai Mountains) economic management areas, and it accounts for a very small proportion of the total Changbai Mountain area and eventually leads to smaller ISLI values. The ISLI values of water body are the smallest and the average value is 0.1, indicating that its spatial distribution is the most dispersed and its proximity to other land object types is the highest. Thus, ISLI provides more comprehensive information about landscape patterns than COHESION, LSI, DIVISION, and IJI.

To illustrate the temporal changes in landscape pattern of Changbai Mountain Reserve over 30 years, the corresponding changes in ISLI values every 5 years are shown in Figure 10. The maximum increase in ISLI is 0.186, which is shown in Figure 10a. The change is the increase in the ISLI for needleleaf forest. Although the area of needleleaf forest increased rapidly during this period, it was still not comparable to broadleaf forest in terms of landscape dominance. From 2000 to 2020, the changes of the ISLI values did not change significantly. The decrease in ISLI has a maximum value of -0.320, which is shown in Figure 10f. The reduction is caused by the ISLI values of broadleaf forest, leading to a shift in the dominant landscape type, from broadleaf forest to needleleaf forest, and the year 2020 was a very important turning point. This conclusion cannot be drawn using conventional landscape metrics.

In comparison to conventional landscape metrics selected for use in this research, the proposed ISLI not only provides additional information about landscape pattern dynamics but also helps to determine prominent landscape characteristics. For example, although the original land cover maps for 1995 to 2020 showed a steady decline in the area of broadleaf forest, the values of ISLI increased and then decreased (the key turning point was the year 2010) and were still the largest values until 2020, i.e., PLAND was insufficient for identifying dominant landscape types. In addition, although they comprise a larger overall area than impervious surface, the ISLI values of cropland are lower than those of impervious surface, because cropland has a smaller spatial correlation range and more complex spatial information, as indicated by the range parameters of cropland. Furthermore, the values of ISLI can distinguish between broadleaf forest, needleleaf forest, and water bodies, and it is hoped that the synthesis of ISLI and common landscape metrics could be incorporated in accuracy-predictive mapping and improve prediction results in land cover change. However, the ISLI values obtained for land cover types with high DIVISION and low PLAND values will be small and may be insufficient to capture the influences of other

selected landscape metrics (such as IJI and COHESION) because DIVISION and PLAND are the most crucial factors to consider (as shown in Table 3) when interpreting the proposed landscape index.

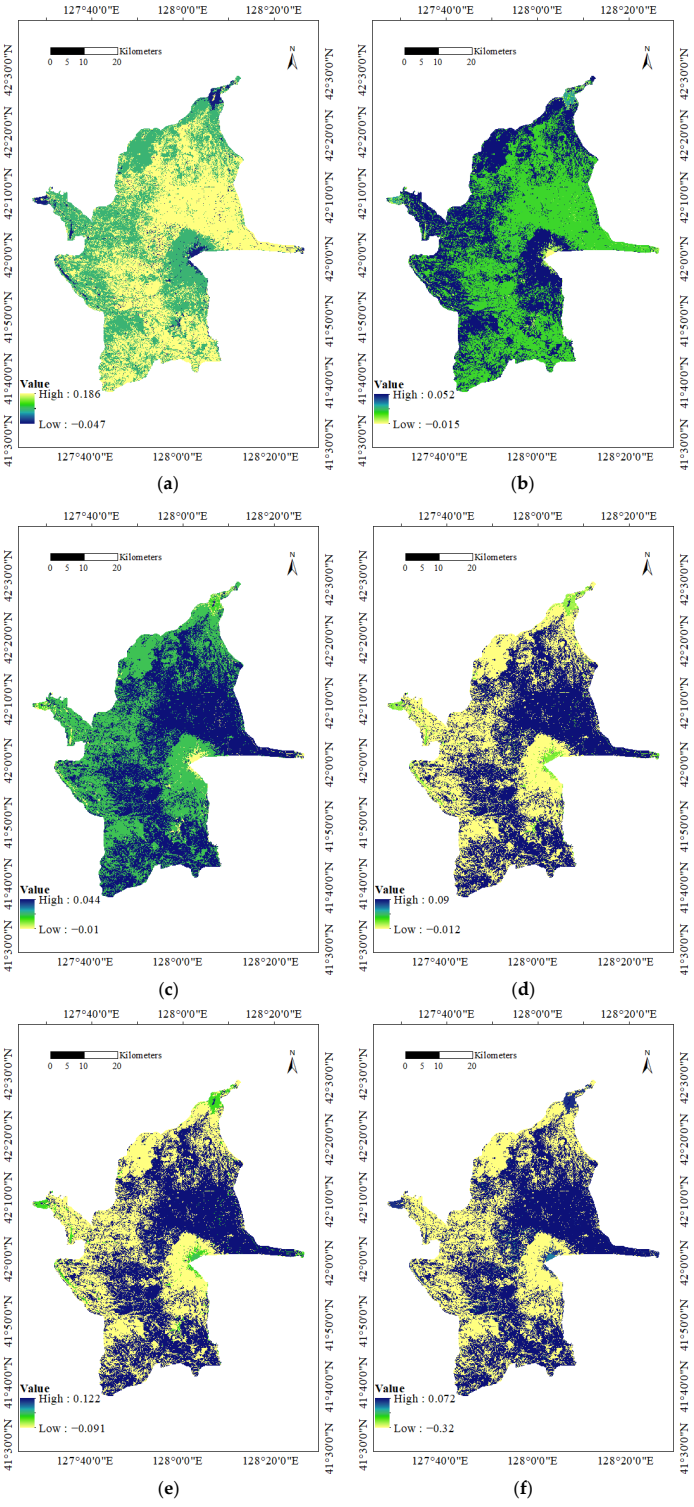

Figure 10. Changes of ISLI values in the Changbai Mountain Reserve from 1995 to 2025: (**a**) from 1995 to 2000, (**b**) from 2000 to 2005, (**c**) from 2005 to 2010, (**d**) from 2010 to 2015, (**e**) from 2015 to 2020, and (**f**) from 2020 to 2025.

In the introductory section, we mentioned the shortcomings of some of the conventional composite metrics in the literature, such as LEI [6], ILI [17], and LFI [18]. They were built differently and meant to serve different purposes or to be used for different landscapes. LEI was proposed to identify types of urban expansion and used buffer analysis to specify distances around the target geographic features. Clearly, it has little in common with the conventional landscape metrics used in the paper for constructing ISLI. As ILI was constructed directly from TA, LSI, PD, and COHESION without applying Pearson's correlation analysis, it may be compared with these conventional landscape metrics. However, these metrics were found to be ineffective for our study, based on the results in Appendix D. For LFI, nine experts were invited to give guidance on assigning proper weights. This is not the case for ISLI, for which expert opinions were not sought. Nevertheless, comprehensive comparisons between ISLI and conventional composite metrics should be undertaken in future research.

Different ecogeographic zones are typically used to examine the consistency of landscape pattern metrics. If the zones have comparable landscape patterns, the conventional landscape metrics and ISLI for related land cover types should be similar. The approach suggested for ISLI is applicable even when different landscape metrics are chosen for regions with various dominant landscapes, although the weights assigned are likely different, resulting in different ISLI values.

Given that the proposed ISLI was only tested in one study area in this research, we will analyze consistency issues in further research. Additionally, we will further analyze the changes in landscape index in terms of scale and extent, index consistency in landscapes and time, the generalizability of weights for constructing ISLI, and the application of geostatistics for landscape pattern research to analyze the Changbai Mountain National Nature Reserve ecosystem more comprehensively.

4. Conclusions

This study analyzed the spatiotemporal changes in the Changbai Mountain National Nature Reserve over a period of 30 years. It was carried out using a variety of conventional landscape pattern indices and the proposed metric ISLI to characterize landscape pattern changes more comprehensively. ISLI was computed using an entropy-based weighting of conventional landscape pattern metrics selected to construct ISLI, while the weighting was based on variogram modelling and correlation analysis between the conventional landscape pattern metrics incorporated and their variogram range parameters. Clearly, the spatial structure information was accounted for when formulating the proper weighting of the conventional landscape metrics considered for constructing ISLI.

The main findings are as follows:

(1) Correlation analysis and significance test results confirm that the correlation between landscape pattern metrics and range parameters is significant, indicating the validity of using spatial structure information for weighting conventional landscape pattern metrics in formulating ISLI. In terms of the range parameters of different land cover types, broadleaf forest and needleleaf forest have much larger range values than those of other land cover types.

(2) DIVISION and PLAND, two of the conventional landscape metrics incorporated into the construction of ISLI, had the greatest weights when calculating ISLI for this study.

The proposed ISLI provides more detailed information than conventional landscape metrics. It comprehensively describes the landscape pattern changes of the dominant landscape over a 30 year period. It is a valuable composite landscape pattern metric, extending and complementing conventional landscape pattern metrics.

Author Contributions: Y.Z., the principal author, contributed mostly to the literature survey in the fields of landscape patterns and remote sensing. Y.Z. was also responsible for research-related experimentation, results analysis and interpretation, and the writing of the paper. The primary contribution of J.Z., the corresponding author, includes the literature review, research design, and paper revision. F.W. reorganized the paper's structure. W.Y. helped with experimentation. All authors have read and agreed to the published version of the manuscript.

Funding: Open Access Funding provided by Jilin University. The project was funded by the National Natural Science Foundation of China (Grants No. 41820104001 and No. 42077242) and the National Key Research and Development Program of China (Grant No. 2020YFA0714103).

Data Availability Statement: The datasets generated during and/or analyzed during the current study are available from the first author on reasonable request.

Acknowledgments: The comments and suggestions from anonymous reviewers, as well as those from an anonymous reviewer for a previous manuscript concerning landscape patterns, were greatly appreciated.

Conflicts of Interest: The authors declare no conflict of interest.

Appendix A. Transition Matrices

Table A1. Transition Matrices of Changbai Mountain from 1995 to 2020 (Unit: km^2).

		2000							
	Land cover type	Cropland	Broadleaf forest	Needleleaf forest	Mixed leaf forest	Impervious surface	Water body	Area changes	Percentage changes
1995	Cropland	36.90	11.39	1.24	0.00	0.38	0.33	13.35	26.6%
	Broadleaf forest	12.42	1701.84	399.09	0.10	0.03	0.35	412.00	19.5%
	Needleleaf forest	0.04	65.16	770.72	0.03	0.00	0.03	65.26	7.8%
	Mixed leaf forest	0.00	0.00	0.00	0.00	0.00	0.00	0.01	100%
	Impervious surface	0.00	0.00	0.00	0.00	11.79	0.00	0.00	0.0
	Water body	0.04	0.29	0.23	0.00	0.00	4.84	0.56	10.4%
		2005							
	Land cover type	Cropland	Broadleaf forest	Needleleaf forest	Mixed leaf forest	Impervious surface	Water body	Area changes	Percentage changes
2000	Cropland	31.79	15.71	0.65	0.00	1.17	0.08	17.61	**35.7%**
	Broadleaf forest	9.10	1587.68	179.66	1.96	0.03	0.25	191.00	10.7%
	Needleleaf forest	1.03	166.35	997.97	5.85	0.00	0.08	173.32	14.8%
	Mixed leaf forest	0.00	0.03	0.10	0.01	0.00	0.00	0.13	92.9%
	Impervious surface	0.00	0.00	0.00	0.00	12.20	0.00	0.00	0.0%
	Water body	0.35	0.29	0.17	0.00	0.01	4.75	0.81	14.6%
		2010							
	Land cover type	Cropland	Broadleaf forest	Needleleaf forest	Mixed leaf forest	Impervious surface	Water body	Area changes	Percentage changes
2005	Cropland	29.20	10.04	0.71	0.00	1.89	0.43	13.07	30.9%
	Broadleaf forest	9.68	1555.34	198.98	5.46	0.31	0.29	214.72	12.1%
	Needleleaf forest	0.39	92.25	1070.42	15.35	0.00	0.15	108.13	9.2%
	Mixed leaf forest	0.00	1.23	5.26	1.33	0.00	0.00	6.49	83.0%
	Impervious surface	0.00	0.00	0.00	0.00	13.40	0.00	0.00	0.0%
	Water body	0.06	0.11	0.27	0.00	0.00	4.73	0.44	8.5%

Table A1. *Cont.*

		2015							
	Land cover type	Cropland	Broadleaf forest	Needleleaf forest	Mixed leaf forest	Impervious surface	Water body	Area changes	Percentage changes
2010	Cropland	29.57	6.83	0.48	0.00	2.30	0.14	9.76	24.8%
	Broadleaf forest	17.65	1447.24	190.78	2.38	0.62	0.30	211.72	12.8%
	Needleleaf forest	1.24	93.34	1171.46	9.32	0.03	0.25	104.18	8.2%
	Mixed leaf forest	0.00	2.20	18.92	1.02	0.00	0.00	21.12	95.4%
	Impervious surface	0.00	0.00	0.00	0.00	15.61	0.00	0.00	0.0%
	Water body	0.23	0.15	0.09	0.00	0.01	5.10	0.49	8.8%
		2020							
	Land cover type	Cropland	Broadleaf forest	Needleleaf forest	Mixed leaf forest	Impervious surface	Water body	Area changes	Percentage changes
2015	Cropland	36.32	8.42	0.91	0.00	2.66	0.39	12.38	25.4%
	Broadleaf forest	16.31	1217.63	313.19	2.27	0.16	0.21	332.14	21.4%
	Needleleaf forest	5.71	93.63	1259.51	22.74	0.01	0.14	122.23	8.8%
	Mixed leaf forest	0.00	1.42	9.90	1.39	0.00	0.00	11.32	89.1%
	Impervious surface	0.03	0.00	0.00	0.00	18.53	0.01	0.04	2.1%
	Water body	0.22	0.28	0.09	0.00	0.01	5.19	0.60	10.4%

Appendix B. Land Cover Prediction in 2025

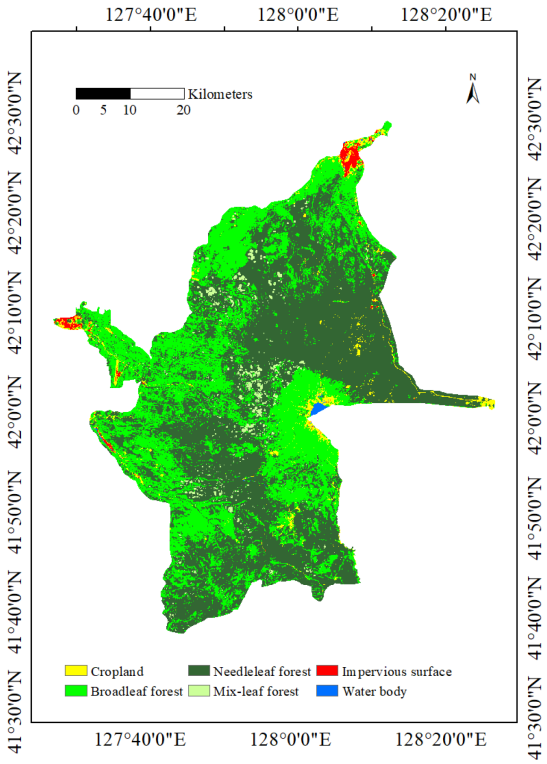

Figure A1. Land cover prediction of Changbai Mountain Reserve in 2025.

Appendix C. Summary Table of Landscape Index

Table A2. Summary Table of Landscape Index.

Area and Edge metrics	Total (class) area (CA); percentage of landscape (PLAND); number of patches (NP); patch density (PD); largest patch index (LPI); total edge (TE); edge density (ED)
Shape metrics	Landscape shape index (LSI); mean patch shape index (SHAPE_MN); area-weighted mean patch shape index (SHAPE_AM); mean patch fractal dimension (FRAC_MN); area-weighted mean patch fractal dimension (FRAC_AM); mean perimeter-area ratio (PARA_MN); perimeter-area ratio area-weighted mean (PARA_AM); perimeter-area fractal dimension (PAFRAC)
Aggregation metrics	Landscape division index (DIVISION); splitting index (SPLIT); effective mesh size (MESH); interspersion and juxtaposition index (IJI); percentage of like adjacencies (PLANDJ); aggregation index (AI); patch cohesion index (COHESION)

Appendix D. Pearson Correlation Coefficients of Landscape Metrics

Table A3. Pearson Correlation Coefficients of the Area and Edge Metrics.

Index	CA	PLAND	NP	PD	LPI	TE	ED
CA	1	1.00 **	0.819 *	0.819 *	0.967 **	0.994 ***	0.994 **
PLAND		1	0.819 *	0.819 *	0.967 **	0.994 **	0.994 **
NP			1	1.00 **	0.864 *	0.869 *	0.869 *
PD				1	0.864 *	0.869 *	0.869 *
LPI					1	0.981 **	0.981 **
TE						1	1.00 **
ED							1

** The correlation is significant at the 0.01 level (double tail); * The correlation is significant at the 0.05 level (double tail).

Table A4. Pearson's Correlation Coefficients of the Shape Metrics.

Index	LSI	SHAPE_MN	SHAPE_AM	FRAC_MN	FRAC_AM	PARA_MN	PARA_AM
LSI	1	−0.098	0.771	−0.181	0.59	0.283	0.143
SHAPE_MN		1	0.383	0.985 **	0.672	−0.94 9 **	−0.864 *
SHAPE_AM			1	0.342	0.891 *	−0.351	−0.499
FRAC_MN				1	0.591	−0.978 **	−0.905 **
FRAC_AM					1	−0.551	−0.631
PARA_MN						1	0.956 **
PARA_AM							1

** The correlation is significant at the 0.01 level (double tail); * The correlation is significant at the 0.05 level (double tail).

Table A5. Pearson's Correlation Coefficients of the Aggregation Metrics.

Index	DIVISION	SPLIT	MESH	IJI	PLANDJ	AI	COHESION
DIVISION	1	0.321	−1.000 **	0.560	−0.472	−0.461	−0.428
SPLIT		1	−0.321	−0.318	−0.946 **	−0.946 **	−0.989 **
MESH			1	−0.560	0.472	0.461	0.429
IJI				1	0.147	0.158	0.175
PLANDJ					1	1.000 **	0.954 **
AI						1	0.952 **
COHESION							1

** The correlation is significant at the 0.01 level (double tail); * The correlation is significant at the 0.05 level (double tail).

Appendix E. Variogram Diagrams

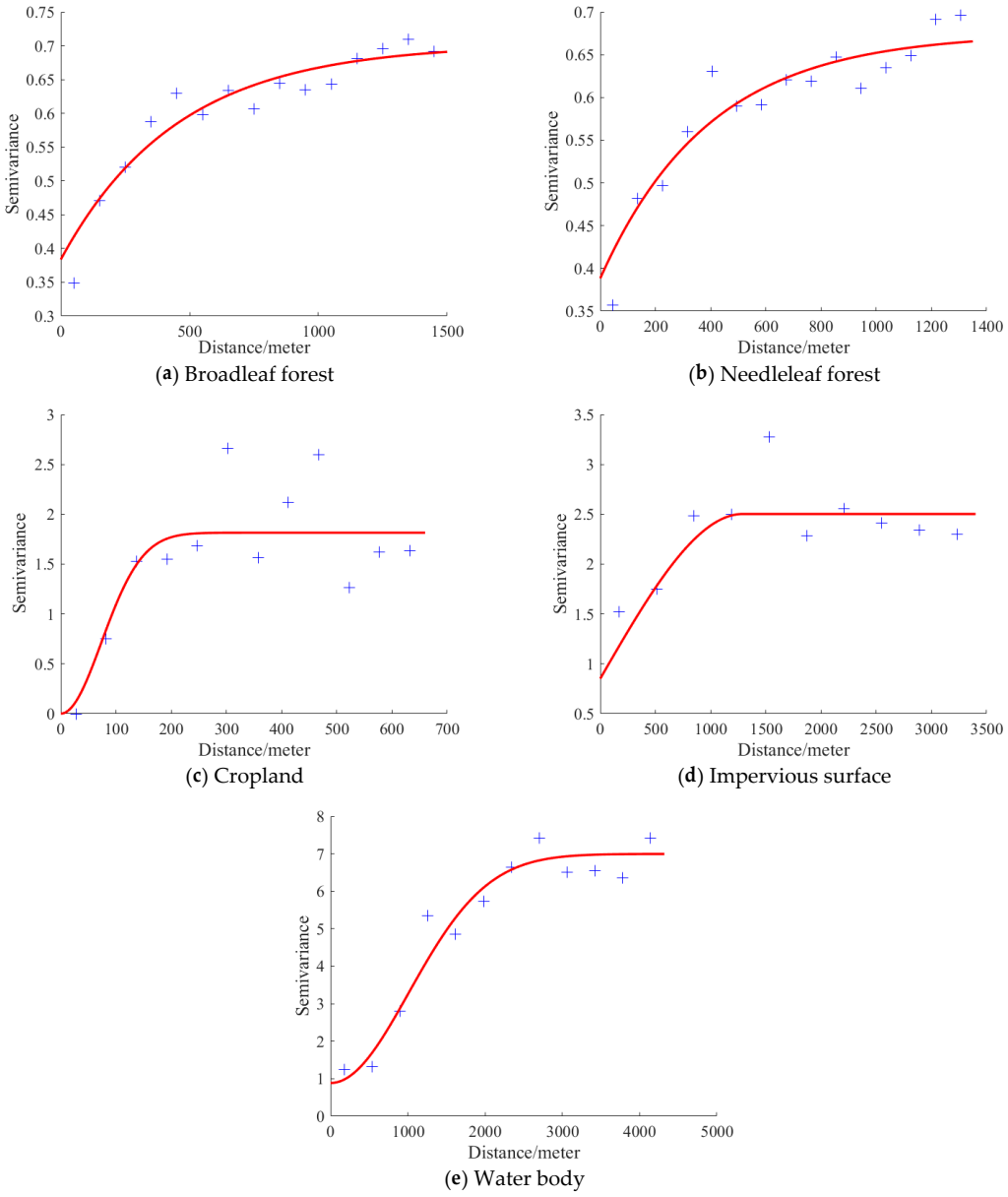

Figure A2. Variogram Diagrams of Different Land Cover Types in 2020.

References

1. Garrigues, S.; Allard, D.; Baret, F.; Weiss, M. Quantifying spatial heterogeneity at the landscape scale using variogram models. *Remote Sens. Environ.* **2006**, *103*, 81–96. [CrossRef]
2. Lv, J.J.; Ma, T.; Dong, Z.W.; Yao, Y.; Yuan, Z.H. Temporal and Spatial Analyses of the Landscape Pattern of Wuhan City Based on Remote Sensing Images. *ISPRS Int. J. Geo-Inf.* **2018**, *7*, 340. [CrossRef]
3. Turner, M.G. Landscape Ecology: What Is the State of the Science? *Annu. Rev. Ecol. Evol. Syst.* **2005**, *36*, 319–344. [CrossRef]
4. Uuemaa, E.A.; Antrop, M.B.; Roosaare, J.C.; Marja, R.C.; Mander, Ü.A. Landscape Metrics and Indices: An Overview of Their Use in Landscape Research. *Living Rev. Landsc. Res.* **2009**, *3*, 1–28. [CrossRef]
5. Wu, J. *Landscape Ecology*; Higher Education Press: Beijing, China, 2007.
6. Liu, X.; Li, X.; Chen, Y.; Tan, Z.; Li, S.; Ai, B. A new landscape index for quantifying urban expansion using multi-temporal remotely sensed data. *Landsc. Ecol.* **2010**, *25*, 671–682. [CrossRef]
7. Turner, M.G. Spatial and temporal analysis of landscape patterns. *Landsc. Ecol.* **1990**, *4*, 21–30. [CrossRef]
8. Wagner, H.H.; Fortin, M.-J. Spatial Ananlysis of Landscapes: Concepts and Statistics. *Ecology* **2005**, *86*, 1975–1987. [CrossRef]
9. Frazier, A.E.; Kedron, P. Landscape Metrics: Past Progress and Future Directions. *Curr. Landsc. Ecol. Rep.* **2017**, *2*, 63–72. [CrossRef]

10. Mander, Ü. Landscape Planning. In *Encyclopedia of Ecology*; Jørgensen, S.E., Fath, B.D., Eds.; Academic Press: Oxford, UK, 2008; pp. 2116–2126.
11. Sang, K.; Fontana, G.L.; Piovan, S.E. Assessing Railway Landscape by AHP Process with GIS: A Study of the Yunnan-Vietnam Railway. *Remote Sens.* **2022**, *14*, 603. [CrossRef]
12. Yu, X.; Mu, C.; Zhang, D. Assessment of land reclamation benefits in mining areas using fuzzy comprehensive evaluation. *Sustainability* **2020**, *12*, 2015. [CrossRef]
13. Gong, J.; Jin, T.; Cao, E.; Wang, S.; Yan, L. Is ecological vulnerability assessment based on the VSD model and AHP-Entropy method useful for loessial forest landscape protection and adaptative management? A case study of Ziwuling Mountain Region, China. *Ecol. Indic.* **2022**, *143*, 109379. [CrossRef]
14. Tian, W.; Xu, Y.; Huang, Y. Comparative analysis of AHP and entropy weight method in urban street landscape evalution. *J. Southwest China Norm. Univ. Nat. Sci. Ed.* **2020**, *45*, 147–153.
15. Shannon, C.E. A Mathematical Theory of Communication. *Bell Syst. Tech. J.* **1948**, *27*, 379–423. [CrossRef]
16. Xia, M.; Jia, K.; Zhao, W.; Liu, S.; Wei, X.; Wang, B. Spatio-temporal changes of ecological vulnerability across the Qinghai-Tibetan Plateau. *Ecol. Indic.* **2021**, *123*, 107274. [CrossRef]
17. Zhang, J.; Yang, X.; Wang, Z.; Zhang, T.; Liu, X. Remote Sensing Based Spatial-Temporal Monitoring of the Changes in Coastline Mangrove Forests in China over the Last 40 Years. *Remote Sens.* **2021**, *13*, 1986. [CrossRef]
18. Zou, L.; Wang, J.; Bai, M. Assessing spatial–temporal heterogeneity of China's landscape fragmentation in 1980–2020. *Ecol. Indic.* **2022**, *136*, 108654. [CrossRef]
19. Wang, H.; Xu, J.; Sheng, L.; Ma, L.; Liu, X. Study on the characteristics of climate change in Changbai Mountain National Natural Reserve from 1958 to 2017. *Arab. J. Geosci.* **2020**, *13*, 1–16. [CrossRef]
20. Zheng, D.; Wallin, D.O.; Hao, Z. Rates and patterns of landscape change between 1972 and 1988 in the Changbai Mountain area of China and North Korea. *Landsc. Ecol.* **1997**, *12*, 241–254. [CrossRef]
21. Liu, L.; Zhang, X.; Gao, Y.; Chen, X.; Mi, J. Finer-Resolution Mapping of Global Land Cover: Recent Developments, Consistency Analysis, and Prospects. *J. Remote Sens.* **2021**, *2021*, 1–38. [CrossRef]
22. Gong, P.; Wang, J.; Yu, L.; Zhao, Y.; Chen, J. Finer resolution observation and monitoring of global land cover: First mapping results with Landsat TM and ETM+ data. *Int. J. Remote Sens.* **2013**, *34*, 2607–2654. [CrossRef]
23. Chen, J.; Chen, J.; Liao, A.; Cao, X.; Chen, L.; Chen, X.; He, C.; Han, G.; Peng, S.; Lu, M. Global land cover mapping at 30 m resolution: A POK-based operational approach. *ISPRS J. Photogramm. Remote Sens.* **2015**, *103*, 7–27. [CrossRef]
24. Soltanikazemi, M.; Minaei, S.; Shafizadeh-Moghadam, H.; Mahdavian, A. Field-scale estimation of sugarcane leaf nitrogen content using vegetation indices and spectral bands of Sentinel-2: Application of random forest and support vector regression. *Comput. Electron. Agric.* **2022**, *200*, 107130. [CrossRef]
25. Wang, G.; Gertner, G.; Xiao, X.; Wente, S.; Anderson, A.B. Appropriate plot size and spatial resolution for mapping multiple vegetation types. *Photogramm. Eng. Remote Sens.* **2001**, *67*, 575–584.
26. Meer, F.V.D. Remote-sensing image analysis and geostatistics. *Int. J. Remote Sens.* **2012**, *33*, 5644–5676. [CrossRef]
27. Asmat, A.; Atkinson, P.M.; Foody, G.M. Geostatistically estimated image noise is a function of variance in the underlying signal. *Int. J. Remote Sens.* **2010**, *31*, 1009–1025. [CrossRef]
28. Garrigues, S.; Verhoef, A.; Blyth, E.; Wright, A.; Balan-Sarojini, B.; Robinson, E.; Dadson, S.; Boone, A.; Boussetta, S.; Balsamo, G. Capability of the variogram to quantify the spatial patterns of surface fluxes and soil moisture simulated by land surface models. *Prog. Phys. Geogr.* **2021**, *45*, 279–293. [CrossRef]
29. Zhang, B.; Zhang, Q.; Feng, C.; Feng, Q.; Zhang, S. Understanding Land Use and Land Cover Dynamics from 1976 to 2014 in Yellow River Delta. *Land.* **2017**, *6*, 20. [CrossRef]
30. Behera, M.D.; Borate, S.N.; Panda, S.N.; Behera, P.R.; Roy, P.S. Modelling and analyzing the watershed dynamics using Cellular Automata (CA)–Markov model–A geo-information based approach. *J. Earth Syst. Sci.* **2012**, *121*, 1011–1024. [CrossRef]
31. Li, l.; Wu, D.; Liu, Y.; Gong, J.; Liu, H.; Zheng, J. Spatial and temporal evolution characteristics and simulation prediction of ecological and economics coordination degree in Huizhou based on a CA-Marcov model. *J. Ecol. Rural Environ.* **2020**, *36*, 161–170.
32. Yin, X. Study on Spatial and Temporal Differentiation Characteristics of Urban Greening 3D Landscape Pattern Based on GIS. Master's Thesis, Liaoning Normal University, Dalian, China, 2019.
33. McGarigal, K.; Markds, B. FRAGSTATS 4.2: Spatial Pattern Analysis Program for Categorical Maps. Available online: https://github.com/kmcgarigal/Fragstats (accessed on 15 January 2022).
34. Riitters, K.H. A factor analysis of landscape pattern and structure metrics. *Landsc. Ecol.* **1995**, *10*, 23–39. [CrossRef]
35. Asuero, A.G.; Sayago, A.; Gonzalez, A. The correlation coefficient: An overview. *Crit. Rev. Anal. Chem.* **2006**, *36*, 41–59. [CrossRef]
36. Cui, L.; Luo, C.; Yao, C.; Zou, Z.; Wu, G.; Li, Q.; Wang, X. The Influence of Climate Change on Forest Fires in Yunnan Province, Southwest China Detected by GRACE Satellites. *Remote Sens.* **2022**, *14*, 712. [CrossRef]
37. Bu, R.; Hu, Y.; Chang, Y.; Li, X.; He, H. A correlation analysis on landscape metrics. *Ecol. Sin.* **2005**, *25*, 2764–2775.